

High-Pressure Synthesis and Recovery of Single Crystals of the Metastable Manganese Carbide, MnC_x

Paul V. Marshall,^[a] Scott D. Thiel,^[a] Elizabeth E. Cote,^[a] John Arigbede,^[a]
Matthew L. Whitaker,^[b] and James P. S. Walsh^{*[a]}

Transition metal carbides find widespread use throughout industry due to their high strength and resilience under extreme conditions. However, they remain largely limited to compounds formed from the early d-block elements, since the mid-to-late transition metals do not form thermodynamically stable carbides. We report here the high-pressure bulk synthesis

of large single crystals of a novel metastable manganese carbide compound, MnC_x ($P6_3/mmc$), which adopts the anti-NiAs-type structure with significant substoichiometry at the carbon sites. We demonstrate how synthesis pressure modulates the carbon loading, with ~40% occupancy being achieved at 9.9 GPa.

Introduction

The first-row transition metal carbides (TMCs) are a class of highly resilient materials renowned for their ability to withstand extreme conditions.^[1–3] They are characterized by a unique interplay of covalent, ionic, and metallic bonding, which allows them to excel in high-strength,^[4] high-resilience, and high-refractory applications.^[5]

The majority of the industrially significant TMCs involve early group transition metals, since these elements tend to form highly stable interstitial carbides.^[6] Specifically, the carbides of the Group 4–5 elements readily form in the NaCl-type (B1) structure, where carbon occupies the octahedral voids within an fcc lattice adopted by the metal. The stability of the NaCl-type carbides is correlated to the valence electron contribution of the metal element,^[7] and can be understood within the framework of an increased population of antibonding orbitals as the number of d-electrons is increased.^[8–11] This destabilization effect poses a significant challenge for the bulk synthesis of TMCs with elements to the right of Group 6 in the periodic table,^[6] and synthetic chemists must turn to non-equilibrium processes such as rapid cooling, or to the preparation of thin films or nanoparticles, where surface energy effects dominate.^[12–14]

Manganese belongs to Group 7 and is the third most abundant transition metal in the Earth's crust.^[15] It is used on a large scale as an additive in steels, lending greater strength, workability, and wear resistance.^[16–18] Despite possessing five unpaired electrons, the use of manganese in magnetic applications is surprisingly restricted. The primary limitation

arises from exchange interactions among its nearest neighbors, which cause atomic magnetic moments to align in opposing directions and result in a non-magnetic state.^[19]

Direct exchange between the half-filled d-bands of Mn makes many of its compounds inherently antiferromagnetic, and the hybridization of the nearest-neighbor orbitals serves to further reduce the magnetic moment. This problem has been termed the “manganese dilemma” and is exemplified in the Mn–Al, Mn–Bi, and Mn–Ga systems. The dilemma is that in order to achieve a significant magnetic moment, the manganese atoms must be well separated – but this diminishes its overall magnetism per unit volume. Upon inspection, a clear trend is observed in these systems between Mn–Mn distance and the resulting magnetic properties: Mn–Mn distances below 2.4 Å tend to be nonmagnetic, distances between tend to show small itinerant antiferromagnetic moments, and distances greater than 2.9 Å tend to show larger ferromagnetic moments.^[21] Despite this dilemma, manganese-based permanent magnets are receiving significant attention for their potential to bridge the gap between rare earth magnets and those with much lower maximum energy products such as the ferrites.^[22]

Manganese carbides have recently attracted attention due to their potential magnetic properties, with magnetic ordering having been observed in Mn_{23}C_6 below 104 K,^[23] and computational studies suggesting that the hypothetical 2D manganese carbides could demonstrate the high-temperature ferromagnetism and half-metallicity crucial for spintronic nanodevices.^[24] Furthermore, manganese-based permanent magnets are attractive as a cost-effective and environmentally friendly alternative to rare-earth-based magnets.^[25–27]

The manganese–carbon system poses several practical challenges, particularly concerning the isolation and study of its compounds. Although there is a consensus that a number of stoichiometric manganese carbides exist, there remains a high degree of uncertainty with respect to their phase boundaries. This uncertainty can be attributed to the chemical reactivity of manganese carbides,^[23] as well as the intrinsic metastability of the phases themselves. Indeed, some researchers go as far as to describe all of the known stoichiometric compounds as

[a] P. V. Marshall, S. D. Thiel, E. E. Cote, J. Arigbede, Prof. J. P. S. Walsh
Department of Chemistry, University of Massachusetts Amherst,
Amherst, MA 01003, United States
E-mail: jpswalsh@umass.edu

[b] Dr. M. L. Whitaker
Department of Geosciences, Stony Brook University,
Stony Brook, NY, 11794-2100, United States

Supporting information for this article is available on the WWW under
<https://doi.org/10.1002/chem.202401581>

metastable phases.^[28] Herein we present the high-pressure synthesis and recovery to ambient conditions of single crystals of MnC_x , a novel metastable phase in the manganese–carbon system. Single crystal X-ray diffraction is used to examine the crystal structure, and first-principles methods are used to understand its stability under high pressures.

Methods

We carried out high-pressure and high-temperature synthesis runs in a large volume multi-anvil press. The runs spanned a range of pressures (5.6–9.9 GPa) and precursor C/Mn ratios (0.33, 0.40, and 1.0). In all of the runs, the sample was compressed to the target pressure and then heated to around 1200 K for between 8–10 minutes. After thermally quenching the reactions and then decompressing to ambient conditions, each run yielded a highly crystalline product containing a large number of single crystals with dimensions of up to 100 μm . Single crystal X-ray diffraction was performed on the crystals with sufficient size (above $\sim 20 \mu\text{m}$), and in all cases the crystal structures could be readily solved as MnC adopting the anti-NiAs-type structure with the space group $P6_3/mmc$.

Results and Discussion

The solved crystal structure is shown in Figure 1, and can be described as the anti-NiAs-type with a significant substoichiometry at the carbon site that correlates to the pressure and/or starting composition (vide infra). The anti-NiAs-type is found in several TMCs and is commonly described as the HCP analogue of the NaCl-type structures observed in the early group TMCs. The manganese atoms of the hexagonal phase are arranged in a distorted HCP array, with carbon atoms filling a subset of the octahedral voids. Characterizing the structure in terms of its layer stacking leads to an AcBcAcBc sequence, where the A and B sites form the HCP lattice of the manganese atoms and the c sites constitute a primitive hexagonal sublattice adopted by the carbon atoms.^[29] This differs from a previously reported cubic high-pressure Mn–C phase synthesized under similar conditions.^[30] It is noteworthy here that anti-NiAs-type carbides are frequently substoichiometric and are often characterized by

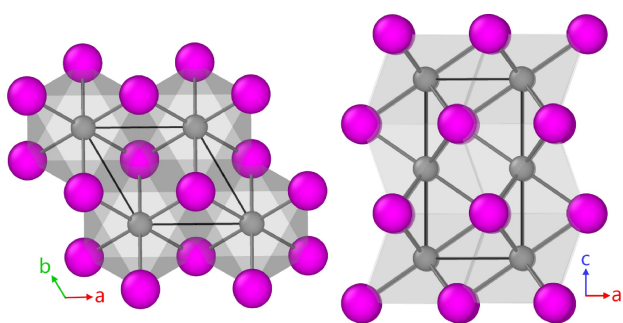


Figure 1. Crystal structure of MnC_x ($P6_3/mmc$) anti-NiAs-type. Manganese and carbon represented with purple (Mn) and grey (C) spheres. Octahedral coordination environments around the carbon atoms are highlighted with grey polyhedra. Image rendered using OVITO.^[20]

ordered vacancies.^[31,32] It is possible that MnC_x also possesses an ordering of the carbon atoms – as we discuss in more detail below – but all 30 datasets reported here were reduced and solved as the anti-NiAs-type described above.

We plot the lattice parameters determined from single crystal X-ray diffraction in Figure 2, which offers a useful proxy for the carbon content (higher carbon content is expected to lead to a higher unit cell volume). We present ten crystals from each of the three runs, plotting each run with separate symbols and colors. The main panel plots the a -axis and c -axis parameters for each crystal. A noticeable grouping emerges that appears to be driven by both pressure and initial reaction composition. The samples recovered from the 9.9 GPa synthesis with precursor C/Mn ratio of 1.0 (i.e. the most carbon rich composition) exhibit the largest unit cell volumes; the samples recovered from the 9.0 GPa synthesis with a C/Mn ratio of 0.33 exhibits smaller lattice parameters; and the 5.6 GPa synthesis with a C/Mn ratio of 0.40 exhibits the smallest cell parameters.

Comparing the lattice parameters of the samples retrieved from the syntheses with the lowest starting carbon concentrations (C/Mn of 0.33 and 0.40), we see that an elevated synthesis pressure (9.0 GPa vs. 5.6 GPa, respectively) yields crystals with a larger unit cell volume, despite having slightly less carbon in the precursor mixture. Thus, pressure is clearly a major driving force in the amount of carbon present in the synthesized phases. However, the composition is also important, as demonstrated by the significantly smaller volume for the 9.0 GPa run as compared to the 9.9 GPa run, where the pressures are similar but the carbon content is reduced by two thirds (C/Mn of 0.33 and 1.0, respectively).

A more direct measure of the carbon content is a refinement of the occupancy at the carbon site against the experimentally observed reflection intensities. We refined this parameter in all of the models, and in all cases observed a lower R -factor when allowing it to refine. All refinements were stable

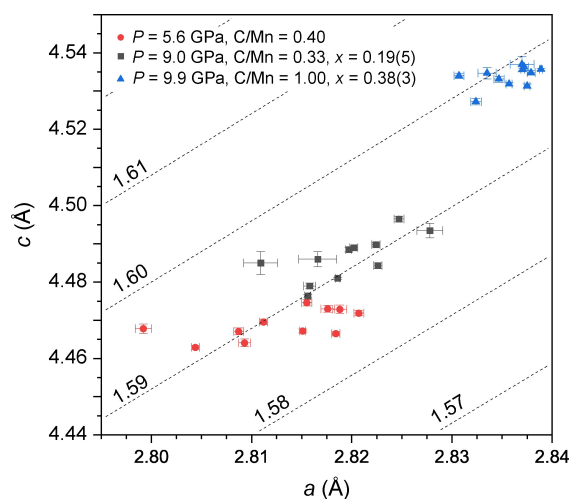


Figure 2. Plot of the a and c lattice parameters of MnC_x of the three experiments. The synthetic pressures, starting composition, and reliable mean occupancies are shown in the legend. Error bars represent the estimated standard deviation reported from indexing. The dashed lines represent the c/a ratio.

and led to values of $0 < x < 1$. It should be noted that the X-ray scattering factor of a light element such as carbon is rather low, which affects the reliability of this parameter as an accurate measure of carbon content, especially when the occupancy is low. Nevertheless, we find a good agreement between the cell volume and the refined occupancy at the carbon site. The mean occupancy value ranges from $x = 0.38(3)$ in the 9.9 GPa synthesis down to $x = 0.18(15)$ in the 5.6 GPa synthesis. The values in the parentheses represent the standard deviation to a 95% confidence level, and we interpret a higher spread of occupancy values to be a reflection of a less reliably constrained occupancy in the crystallographic model for the low-carbon samples. The mean occupancy values are noted in Figure 2, showing a clear correlation with the cell volume. Note that we do not present the mean for the $P = 5.6$ GPa due to the low reliability of this parameter, which arises due to a very low carbon occupancy. The individual values are reported in the Supporting Information for the samples where this could be refined, and these values are consistent with a very low occupancy.

To get a broad sense of the stability of different manganese carbides, we calculated the formation enthalpies of phases known to the Mn–C system as well as to other related transition metal borides, carbides, and nitrides. The resulting convex hull and distances from the hull are plotted in the Supplemental Information. The fully stoichiometric anti-NiAs structure adopting the $P6_3/mmc$ spacegroup has a significantly positive formation enthalpy, while the ordered substoichiometric η -Fe₂N-type Mn₂C ($Pbcn$) is negative and much closer to the hull. The known manganese carbides – which are all metal rich – tend to have much lower formation enthalpies, a finding that is consistent with theory and results from studies of similar carbide systems.^[6,8,14,33]

To gain further insight into how substoichiometry at the carbon site affects stability, we ran calculations over a sampling of substoichiometric space within the anti-NiAs-structure – an approach similar to one we have used previously.^[33] We ran these calculations at 0 GPa and 20 GPa, and the results of these calculations are shown in Figure S3. We observe from the 0 GPa calculations that the stability of the anti-NiAs-structure is significantly affected by substoichiometry. The ideal MnC ($x = 1$) has a positive formation enthalpy of ~ 100 meV, but falls with decreasing carbon content before eventually becoming negative below $x \sim 0.4$. A minimum in the formation enthalpy appears at around $x = 0.30$ (i.e. MnC_{0.3}), where the formation enthalpy is ~ -20 meV. In the 20 GPa calculations, the ideal MnC now has a negative formation enthalpy (~ -10 meV), and again falls with decreasing carbon content to a minimum at around $x = 0.40$ (i.e. MnC_{0.4}), where the formation enthalpy becomes (~ -70 meV). Examining the volume of each of the unit cells (Figure S4), we see a clear correlation between unit cell volume and carbon content, with the volume dropping by around 1/3 between fully stoichiometric MnC and the hypothetical HCP–Mn (no octahedral sites filled). The predominant features of this system are reminiscent of those of the metastable substoichiometric NaCl-type CrC in the Cr–C system, thus bolstering a common theme of metal-rich substoichiome-

tries supporting the synthesis of metastable phases in a system that favors metal-rich stoichiometries.^[33]

To this point, we have described the structure as anti-NiAs-type with a random ordering of vacancies at the carbon site. However, it is commonly seen in other anti-NiAs-type phases that the vacancies are ordered. For example, in tungsten semicarbide, W₂C, an HCP metal sublattice hosts an ordered distribution of carbon, which can occupy approximately 35% to 51% of the octahedral interstices. A total of three ordered phases are known: (1) an orthorhombic ($Pbcn$) B' -W₂C (also known as ζ -W₂C), which adopts the ζ -Fe₂N (Mo₂C) structure; (2) a rhombohedral ($P\bar{3}m1$) B'' -W₂C (also known as α -W₂C), which adopts the anti-CdI₂ structure; and (3) a trigonal ($P\bar{3}1m$) ε -W₂C, which adopts the ε -Fe₂N structure type.

In all three polymorphs, the tungsten lattice is only slightly distorted from an ideal HCP lattice, and the strong scattering factor of tungsten makes it difficult to detect the ordering of the light element carbon. Low-angle reflections can be a signature of a supercell arising from the ordering, but these peaks are often too weak to extract reliable intensities from, complicating the assignment of the structure.^[34]

To look for the presence of any low-angle peaks that were missed by our indexing routine, we merged detector images collected with the same detector positions for selected crystals that exhibited strong diffraction (see Supporting Information). Very weak diffraction spots can be resolved at low angles, suggesting the possibility of unresolved long-range order, and motivating the use of techniques such as neutron diffraction to more accurately determine the crystal structure.

Conclusions

We have presented a combined experimental synthesis and first-principles study of the novel transition metal carbide, MnC_{*x*} ($P6_3/mmc$), which we synthesized under high pressures and temperatures. Recovered single crystals were studied with single-crystal X-ray diffraction and were solved as an anti-NiAs-type structure with a random distribution of vacancies at the carbon site. First-principles methods were employed to study the stabilizing effect of substoichiometric carbon, yielding results consistent with the measured carbon occupancy. Overall, our results show that MnC_{*x*} can host a broad range of carbon in the octahedral sites, and that the carbon amounts can be readily controlled with pressure and composition. Ongoing studies will characterize the bulk properties of this new phase.

Deposition number 2355186 contains the supplementary crystallographic data for this paper. This data is provided free of charge by the joint Cambridge Crystallographic Data Centre and Fachinformationszentrum Karlsruhe Access Structures service.

Acknowledgements

This work was funded by the National Science Foundation (DMR-2237478) and by an American Chemical Society Petro-

leum Research Fund grant (PRF-66490). Portions of this work were performed using resources provided by the Massachusetts Green High Performance Computing Cluster (MGHPCC). This research used resources 28-ID-2 of the National Synchrotron Light Source II, a U.S. Department of Energy (DOE) Office of Science User Facility operated for the DOE Office of Science by Brookhaven National Laboratory under Contract No. DE-SC0012704. Use of the MAXPD endstation was supported by COMPRES, the Consortium for Materials Properties Research in Earth Sciences, under NSF Cooperative Agreement No. EAR 16-61511 and by the Mineral Physics Institute, Department of Geosciences, Stony Brook University. Crystal structures were rendered using OVITO 3.8.3.

Conflict of Interests

The authors declare no conflict of interest.

Data Availability Statement

The data that support the findings of this study are available from the corresponding author upon reasonable request.

Keywords: Keywords: high pressure, multi-anvil press, solid-state synthesis, density functional theory, transition metal carbides

- [1] Y. Xiao, J.-Y. Hwang, Y.-K. Sun, *J. Mater. Chem. A* **2016**, *4*, 10379–10393.
- [2] X. Zang, C. Jian, T. Zhu, Z. Fan, W. Wang, M. Wei, B. Li, M. Follmar Diaz, P. Ashby, Z. Lu, et al., *Nat. Commun.* **2019**, *10*, 3112.
- [3] W. S. Williams, *Prog. Solid State Chem.* **1971**, *6*, 57–118.
- [4] Y. Tan, Z. Teng, C. Chen, P. Jia, X. Zhou, H. Zhang, *Ceram. Int.* **2021**, *47*, 16882–16890.
- [5] E. Coy, V. Babacic, L. Yate, K. Załęski, Y. Kim, J. S. Reparaz, B. Dörling, B. Graczykowski, I. Iatsunskyi, K. Siuzdak, *Chem. Eng. J.* **2021**, *415*, 128987.
- [6] Q. Wang, K. E. German, A. R. Oganov, H. Dong, O. D. Feya, Y. V. Zubavichus, V. Y. Murzin, *RSC Adv.* **2016**, *6*, 16197–16202.
- [7] K. Kaufmann, E. Wenger, K. Vecchio, *Scr. Mater.* **2023**, *229*, 115382.
- [8] S. D. Wijeyesekera, R. Hoffmann, *Organometallics* **1984**, *3*, 949–961.
- [9] I. Khatiri, N. Szymanski, B. Dumre, J. Amar, D. Gall, S. Khare, *J. Alloys Compd.* **2022**, *891*, 161866.
- [10] G. Greczynski, D. Primetzhofer, L. Hultman, *Appl. Surf. Sci.* **2018**, *436*, 102–110.
- [11] T. Das, S. Deb, A. Mookerjee, *Phys. B (Amsterdam Neth.)* **2005**, *367*, 6–18.
- [12] H. Bhadeshia, *Int. Mater. Rev.* **2020**, *65*, 1–27.
- [13] E. Moghaddam, N. Varahram, P. Davami, *Mater. Sci. Eng. A* **2012**, *532*, 260–266.
- [14] P. V. Marshall, Z. Alptekin, S. D. Thiel, D. Smith, Y. Meng, J. P. Walsh, *Chem. Mater.* **2021**, *33*, 9601–9607.
- [15] K. Heinze, *Nat. Chem.* **2021**, *13*, 926–928.
- [16] C. Clarke, S. Upson, *Neurotoxicology* **2017**, *58*, 173–179.
- [17] S. Mohanty, S. Ghosh, B. Bal, A. P. Das, *Rev. Environ. Sci. Bio/Technol.* **2018**, *17*, 791–811.
- [18] R. Jacob, S. R. Sankaranarayanan, S. K. Babu, *Mater. Today: Proc.* **2020**, *27*, 2852–2858.
- [19] J. Kasper, B. Roberts, *Phys. Rev.* **1956**, *101*, 537.
- [20] A. Stukowski, *Modell. Simul. Mater. Sci. Eng.* **2009**, *18*, 015012.
- [21] J. Coey, *J. Phys. Condens. Matter* **2014**, *26*, 064211.
- [22] T. Keller, I. Baker, *Prog. Mater. Sci.* **2022**, *124*, 100872.
- [23] P. Karen, H. Fjellvåg, A. Kjekshus, P. Andresen, *Acta Chem. Scand.* **1991**, *45*, 549–557.
- [24] K. Sheng, Z.-Y. Wang, H.-K. Yuan, H. Chen, *New J. Phys.* **2020**, *22*, 103049.
- [25] T. Keller, D. Barbagallo, N. Sheremetyeva, T. K. Gosh, K. S. Shanks, G. Hautier, I. Baker, *J. Magn. Magn. Mater.* **2024**, *265*, 119646.
- [26] T. Roman, I.-I. Murgulescu, G. Ababei, G. Stoian, M. Lostun, M. Porcescu, M. Grigoras, N. Lupu, *Mater. Today Commun.* **2022**, *33*, 104241.
- [27] T. Keller, I. Baker, *Prog. Mater. Sci.* **2022**, *124*, 100872.
- [28] Y. Liu, T. G. Kelly, J. G. Chen, W. E. Mustain, *ACS Catal.* **2013**, *3*, 1184–1194.
- [29] G.-i. Oya, Y. Onodera, *J. Appl. Phys. (Melville NY U. S.)* **1976**, *47*, 2833–2840.
- [30] A. Arpita Aparajita, N. Sanjay Kumar, S. Chandra, S. Amirthapandian, N. C. Shekar, K. Sridhar, *Inorg. Chem.* **2018**, *57*, 14178–14185.
- [31] A. I. Gusev, A. A. Rempel, A. J. Magerl, *Disorder and order in strongly nonstoichiometric compounds: transition metal carbides, nitrides and oxides, Vol. 47*, Springer Science & Business Media, **2013**.
- [32] N. Schönberg, *Acta Metall.* **1954**, *2*, 427–432.
- [33] P. V. Marshall, S. D. Thiel, E. E. Cote, R. Hrubciak, M. L. Whitaker, Y. Meng, J. P. Walsh, *ACS Mater. Au* **2023**.
- [34] A. Kurlov, A. Gusev, *Phys. Rev. B* **2007**, *76*, 174115.

Manuscript received: April 24, 2024

Accepted manuscript online: May 21, 2024

Version of record online: ■■, ■■